Fluid mechanics of fibre suspensions related to papermaking

RICHARD HOLM

KTH Mechanics

Doctoral Thesis
Stockholm, Sweden 2005

Fluid mechanics of fibre suspensions related to papermaking

by

Richard Holm

December 2004
Doctoral Thesis from
Royal Institute of Technology (KTH)
KTH Mechanics
SE-100 44 Stockholm, Sweden

Typsatt i $\mathcal{AMS}$-LaTeX in MechThesis style.

Akademisk avhandling som med tillstånd av Kungliga Tekniska Högskolan i Stockholm framlägges till offentlig granskning för avläggande av teknologie doktorsexamen fredagen den 14:e januari 2005 kl 10.00 i Kollegiesalen, Administrationsbygnaden, Kungliga Tekniska Högskolan, Stockholm.

©Richard Holm 2004

Edita AB, Stockholm 2004

Fluid mechanics of fibre suspensions related to papermaking

Richard Holm 2004, KTH Mechanics, Royal Institute of Technology
SE-100 44 Stockholm, Sweden.

Abstract

This thesis deals with fluid dynamic mechanisms related to papermaking, specifically: the initial dewatering mechanisms during roll-forming and fibre motion in sedimentation and in shear flow.

Pressure and wire position measurements have been conducted in a model resembling the forming zone and the measured pressure distributions are shown to have more complex patterns than the simple model $p = T/R$ (where T is the wire tension and R is the roll radius). It is shown that an increase in wire tension has a similar effect as a decrease in flow-rate on the shape of the pressure distribution. In addition, it is shown that the drainage has a stabilizing effect on the dewatering pressure.

The flow around the forming roll has also been modelled with the assumption that the wire is impermeable. A non-linear equation for the position of the wire is derived that clearly shows that the Weber number, We, is an important parameter. The equation is linearized around the trivial solution and has a standing wave solution with a specific wavelength that scales with the We-number.

Motion of non-Brownian fibre settling in a Newtonian fluid at a small but finite Reynolds number has been studied experimentally. Two different regimes of sedimentation were identified. For dilute suspensions, fibres generally fall without flipping and may travel at velocities larger than that of an isolated particle. In the semi-dilute regime we found the settling process to be dominated by large-scale fluctuations. The velocity fluctuations scale with the suspension volume concentration ϕ according to $\phi^{1/3}$, which is similar to the findings for settling spheres.

The influence of shear on fibre orientation in the near wall region was studied in cellulose acetate fibre suspensions. At low concentration and low aspect ratio fibres were observed to orient perpendicular to the streamwise direction (named rollers) in the near wall region whereas the orientation further into the suspension was unchanged. As the concentration and aspect ratio increased the fraction of rollers decreased.

Finally, an evaluation of a commercial Ultra Velocity Profiler unit in fibre suspensions are presented. The idea was to determine the velocity and characterise the turbulence from ultra sound echoes from particles in the fluid. However, the spatial and/or temporal resolution of the measurements did not permit turbulence characterisation. These limitations might be possible to overcome and some procedures are proposed and evaluated.

Descriptors: applied fluid mechanics, fibre suspensions, roll-forming, sedimentation, shear flow, ultrasound measurements, papermaking

Preface

Fluid mechanics is a basic science as well as an engineering subject, with applications in many different fields, such as aeronautics, energy conversion, geophysics, biomedical flows, chemical engineering, paper technology etc. Fluid mechanics plays a fundamental role in some of these applications (for example aircraft engineering) and is an important factor in others. The application of fluid mechanics to industrial processes has expanded in the recent years.

The present work deals with some of the fluid dynamics mechanisms involved in papermaking. It is divided into two parts: the initial part, treating dewatering mechanisms during roll forming, and a second part dealing with studies of fibre motion. The work is mainly experimental, using a model of the roll forming section of a paper machine and studying the fibre motion in well-defined flow fields (sedimentation and shear flow). The study of mechanisms related to papermaking is challenging regarding both theoretical and experimental aspects. For example, fibre suspensions are opaque already at small volume concentrations of fibres. To conduct measurements requires for example index-of-refraction matching or using ultrasonic techniques.

The thesis contains two sections, a summary section and a paper section. In the summary, a brief description is given of papermaking, some relevant basic fluid mechanics and aspects regarding fibre suspensions. This is followed by the corresponding papers, that have been reset in the thesis format. Also the figures are adjusted to the format of thesis.

Stockholm, December 2004 *Richard Holm*

"The price of reliability is the pursuit of the utmost simplicity.
It is a price which the very rich find the most hard to pay."

Sir Antony Hoare, 1980

Contents

CHAPTER 1

Papermaking

The art of papermaking originated in China, and has been going on for more than 2000 years. Until the end of the 18^{th} Century, paper was made by hand, one sheet at a time. Today, a modern papermaking machine can produce up to 600,000 tons of paper per year. The basic steps that have to be taken are however similar, as prescribed in a typical handcraft book

- *Take some of your slurry and fill with tap water until you have the proper consistency in the container.*
- *Agitate the mixture in the mould with and up-and-down action rather that a swirling action.*
- *Submerge a mould into the suspension and lift up the mould and level off, gently shake the mould to distribute pulp evenly.*
- *Place the pulp and frame in another sink to allow the water to drain.*
- *Carefully lift off the top wooden frame taking care not to disturb the pulp.*
- *Place a blotting-paper on the pulp layer.*
- *Use a rolling pin to get even more moisture out of the pulp.*
- *Iron the paper pulp dry. Remove the blotting-paper carefully.*
- *If the paper curls you may need to lay it flat under a heavy book for a few days until thoroughly cured*

From these instructions, it is obvious that papermaking is strongly coupled to fluid mechanics: it is a fibre suspension flow (non-Newtonian and dependent on the pulping process); turbulent mixing e.g. for obtaining a homogenous suspension; the sheet forming process (building up a sheet of paper); application of shear flows (shaking) to control the orientation and distribution of the fibres; pressing and drying, which includes mechanical and thermodynamic processes.

The distribution of fibres, fillers and fines in the final paper sheet is quantified as paper formation, *i.e.* as the degree of local basis weight variation. This is one of the most important quality aspects of the final product.

Machines used in modern paper production always consist of the forming section (see Figure 1.1), the press section and a drying section. Depending on the paper (or board) product manufactured other unit processes, such as e.g. coating, can be added but these three are always present. As already mentioned, the basic principles used in making traditional handsheet paper

are still applied in modern papermaking machines. The modern process starts with a fibre suspension, at low concentration[1] of cellulose fibres in water. The concentration is typically between 0.5-1% and the suspension is distributed by a nozzle in what is referred to as the headbox in a form of a plane liquid jet, onto either one or between two permeable bands called wires or forming fabrics. These move at approximately the same speed as the fibre suspension jet coming from the headbox. Initial dewatering (removal of water) is performed by allowing the water to pass through the holes in the forming fabrics while trapping the fibres. Various methods can be used to influence sheet structure and increase dewatering capacity. After initial dewatering of the web, the solids content in the formed web is usually in the region of 12-15%, meaning that $\approx$ 95% of the water has been removed. The headbox and initial dewatering stage is usually referred to as the paper sheet forming process, or forming for short.

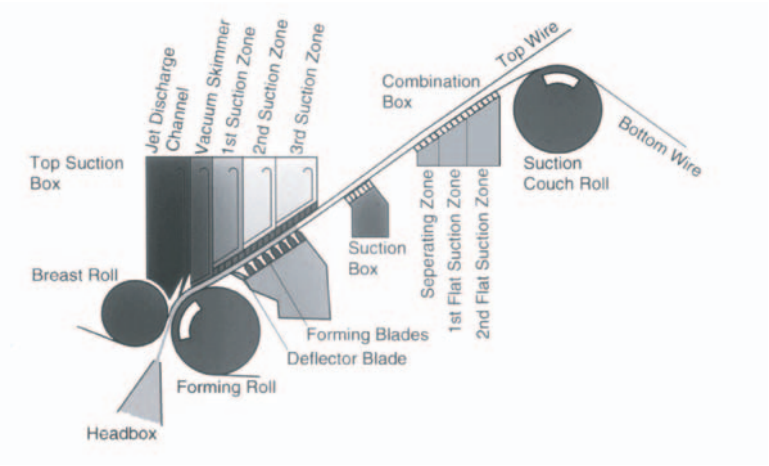

FIGURE 1.1. The roll-blade Duoformer CFD forming unit by Voith.

After forming, the wet web passes through the press section, where further dewatering is performed via mechanical compression in a press nip. This is usually referred to as wet pressing and there are several technical approaches available, though the simplest way is to let the sheet pass between two counter-rotating rolls. The paper sheet is supported by a press-felt as it passes through the nip. The felt also absorbs the water that is mechanically expelled from the wet sheet. The last stage in the manufacturing of paper is to remove the residual water by applying heat, *i.e.* drying. The drying unit is the largest part of a typical papermaking machine.

The papermaking process requires large volumes of water, and is considerably energy intensive. Modern paper mills however use extensive recirculation of water to meet their environmental impact reduction obligations. Nowadays,

[1]Often the word consistency is used but concentration is more accurate.

there are paper mills that use as little as 3 m^3 of water per ton of paper produced, compared to more than 100 m^3 per ton in days gone by.

1.1. The sheet forming process

The heart of the papermaking process is the headbox. The modern headbox typically consists of three parts: the flow distributor or manifold, the tube bank and the nozzle (see Figure 1.2). The fibre suspension is usually fed to the headbox from a perpendicular direction of the nozzle and jet. Usually the flow distributor has a tapered geometry designed to give a constant static pressure across the machine width. This will ensure that the speed of the headbox jet is constant along the width of the paper machine.

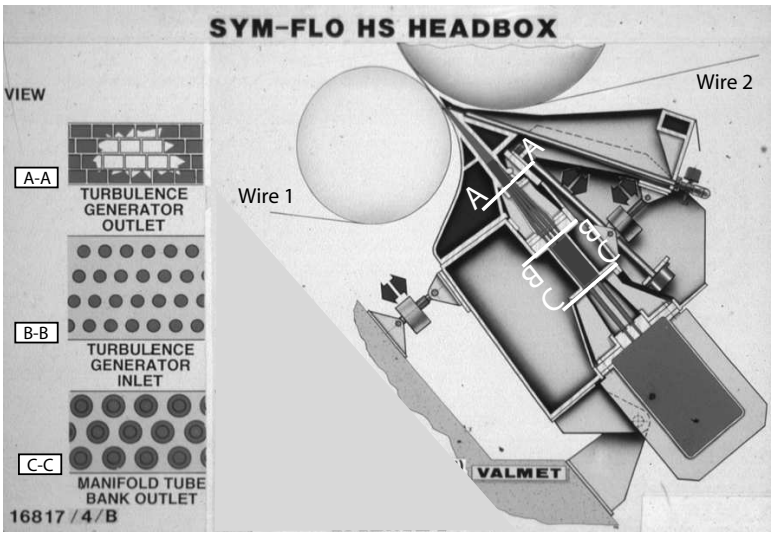

FIGURE 1.2. The Valmet SymFlow HS headbox and the different parts. The cross-sectional view to the left, illustrate the different parts in the headbox.

On exiting the manifold, the fibre suspension enters the tube bank through a system of holes, usually representing around 10% of the area. The main purpose of the tube bank is to produce a pressure drop for promoting a more uniform flow profile across the full width of the papermaking machine. Each flow channel in the tube banks of modern headboxes features a step-diffuser design, see e.g. Hyensjö *et al.* (2004), which results in a defined separation (and turbulence) of the flow, which provides a controlled and elevated pressure drop. The turbulence generated was earlier believed to play an important role in improving the formation in the final paper sheet.

On exiting the tube bank, the suspension flow enters the headbox nozzle accelerating the flow and producing a free plane jet. The flow in the contraction of a headbox has been subject to extensive research, both experimentally (Chuang (1982), Shands (1991), Farrington (1991) and Parsheh (2001)) and numerically (Hua & et. al (1999) and Bandhakavi & Aidun (1999)). Most of these studies have looked at the behaviour of a Newtonian fluids, such as water or air in a headbox contraction. Parsheh (2001) performed measurements and modelled the effect of contraction on turbulence, and concluded that only the most advanced turbulence models can be used to predict flow in headbox contractions, assuming that the effect of the fibres in the suspension is neglected.

Ideally, when the fibre suspension exits the headbox nozzle it is in the form of a two-dimensional plane jet, typically 10 mm thick and up to 10 m wide. This jet impinges on the wire at a narrow angle and at a distance of 10-20 cm downstream the headbox nozzle outlet (often referred to as the headbox slice).

The hydrodynamics of the plane jet has been thoroughly studied by Söderberg (1999), who determined the stability of a plane jet experimentally and theoretically, and showed that the jet was susceptible to two-dimensional wave disturbances. Söderberg was able to observe the breakdown of the waves, which may result in longitudinal (streaky) structures in the jet. Streaky structures can also be seen in the final paper sheets. Söderberg suggested that the streaks in the paper were due to the streaks observed inside the jet.

At impingement the jet speed is close to the wire speed, though a difference may be set intentionally in a real paper machine–either a rush (jet speed greater than wire speed) or a drag (wire speed greater than jet speed)–in order to influence sheet structure and properties. The interaction between the fibre suspension jet and the wires has a clear influence on the surface structure of the paper sheet.

The design of the forming section (or former) of papermaking machines can vary. In its simplest form–as used in the earliest papermaking machines–dewatering is a result of gravity. This is usually referred to as fourdrinier forming, after the Fourdrinier brothers Henry and Sealy, who designed the first papermaking machine. Here the jet lands on one horizontal wire, supported from below on what is called the forming table. An early development of this was the introduction of forced dewatering using local suction below the wire, as well as generating additional activity (pulsations and shear) on the forming table using foils (deflector blades), or even by horizontally shaking the forming table mechanically.

In contrast to single wire forming, twin-wire forming (also called gap-forming) involves the fibre suspension being enclosed between two wires in a sandwich-like design. This symmetrical, wire-suspension-wire sandwich results in a quadrupling of the dewatering capacity compared with single wire forming. Twin-wire forming also has the potential to produce a more symmetric sheet.

If the wire-suspension-wire sandwich is deflected mechanically the wire tension produces an increase in the pressure between the wires, thus enhancing

dewatering. This can be achieved by pressing a "forming" roll or deflector blades against the wire-sheet-wire sandwich from one side (see Norman (1989), this is called roll forming or blade-forming respectively. Additionally, the localised pressure pulses created by the blades in blade forming have a significant influence on the sheet structure. If used properly, they can break-up fibre flocs and improve paper formation. In principle, pressure pulses always have a detrimental effect on the strength of the sheet.

These days there are pure fourdrinier forming units, hybrid forming units (combinations of fourdrinier and twin-wire forming units), and twin-wire forming units in use, with the majority of these being fourdrinier or hybrid units. The most modern paper machines use a combination of roll forming followed by blade forming and the cost for obtaining one of these (paper machine only) is in the range of 2,000,000 Euro ($2,600,000) depending on paper grade.

Recently a numerical model of the forming section was presented by Turnbull *et al.* (1997), which was improved with a two-dimensional approach by Chen *et al.* (1998). A similar model was presented by Zahrai (1997) that could estimate the pressure and wire position in both roll and blade forming and her result showed a possibility of a standing wave solution. Blade forming was also the subject in the numerical work presented by Holmqvist (2002), aimed at the interference between pressure pulses originating from a series of blades. A numerical study by Dalpke (2002), looking at the initial impingement zone in roll forming, showed agreement with experimental data by Gooding *et al.* (2001). For an overview of the area see Malashenko & Karlsson (2000), and also the extensive review by Norman & Söderberg (2001), covering recent developments in paper forming. Some very recent studies of floc behaviour in the forming zone have been presented by Bergström (2003) and Åkesson (2004).

CHAPTER 2

Fluid mechanics

In general, the motion of a Newtonian fluid such as water or air, is given by Navier-Stokes equations. Together these equations constitute one scalar and one vector equation; resulting in four coupled, partial differential equations for pressure (which is a scalar variable), and velocity (which is a vector variable with three components). However these coupled equations are non-linear, which means that the system is mathematically difficult to solve. Though analytical solutions do exist for a number of generic cases, they mostly have to be solved numerically. Because of this, physical observations from experiments or nature still play an important part in fluid mechanics. The Navier-Stokes equations are represented as follows

$$\frac{\partial \mathbf{u}}{\partial t} + \mathbf{u} \cdot \nabla \mathbf{u} = -\frac{1}{\rho}\nabla p + \nu \nabla^2 \mathbf{u} + \frac{1}{\rho}\mathbf{F}, \tag{2.1}$$

where $\mathbf{u} = u\mathbf{e}_x + v\mathbf{e}_y + w\mathbf{e}_z$ is the velocity vector with its three components (u, v, w) and p is the pressure. The parameters are $\nu = \mu/\rho$, which is the kinematic viscosity, where μ is the dynamic pressure and ρ the density. The last term $\mathbf{F}$ represents a volumetric force (for example gravity), which can be neglected in some problems ($\mathbf{F} = 0$). The terms on the left-hand side of the equation is due to the acceleration of the fluid, also referred to as inertia terms, whereas on the right-hand side of the equation the first term is the pressure gradient (force), and the second term represents viscous forces. The continuity equation is expressed as

$$\frac{\partial \rho}{\partial t} + \nabla \cdot \rho \mathbf{u} = 0. \tag{2.2}$$

When this system of equations is to be solved, initial and boundary conditions are needed. A boundary condition occurring frequently is a rigid, impermeable, or solid wall. This condition implies that no fluid is able to pass through the wall, and consequently the wall normal velocity is zero. Additionally, the two other components (parallel to the wall) are also zero. This boundary condition is usually referred to as a no-slip condition. There are other types of boundaries such as free surfaces and permeable walls with constant or variable permeability. Each of these has to be treated appropriately when solving the equations.

Frequently some simplifications are introduced to facilitate solving these equations. In Equations 2.1 and 2.2, the fluid density (ρ) is assumed to be constant. The flow is then said to be incompressible–a simplification often made in regard to liquids. If both pressure and velocity are constant in time, this is referred to as a steady state condition. Furthermore, nature is three-dimensional, but in some flow cases, reducing the problem to one or two dimensions can be justified, further simplifying the equations.

A useful concept when studying fluid flows is that of the dynamic similarities. A flow that at first appeared different but under same circumstances exhibit the same pattern is called dynamically similar. This can be revealed if the variables in the equations are scaled in an appropriate way. This often result in non-dimensional groups and the most famous example is the Reynolds number (Re), expressing the ratio between inertia and viscous forces for Newtonian fluids.The Reynolds number is defined as

$$Re = \frac{\rho U L}{\mu}, \tag{2.3}$$

where U and L are the characteristic velocity and length scales respectively. The Reynolds number can be derived by scaling the Navier-Stokes equations, resulting in

$$\frac{\partial \mathbf{u}}{\partial t} + \mathbf{u} \cdot \nabla \mathbf{u} = -\nabla p + \frac{1}{Re}\nabla^2 \mathbf{u} + \frac{1}{Fr}\mathbf{F}. \tag{2.4}$$

Another non-dimensional number appears in Equation 2.4, namely the Froude number (Fr), which represents the ratio of inertial to volumetric forces. This is for example relevant in bouyancy driven flows, and defined as

$$Fr = \frac{U}{(gL)^{1/2}}, \tag{2.5}$$

where g is the gravitational acceleration. Another non-dimensional number is the Weber number (We), which is useful for characterising fluid flow where there is an interface between two immiscible fluids, for example water and air. The Weber number is defined as

$$We = \frac{\rho U^2 L}{T}, \tag{2.6}$$

where T is the surface tension.

The Péclet number (Pe) express the relationship between the transport of material (convection) by the fluid and the diffusivity. Diffusivity can be of different physical origin, such as thermal or rotary diffusivity, and in the latter case is seen as random (or Brownian) motion. This flexibility has advantages in characterising the flow motion under influence of different mechanisms in the flow. The following definition of the Péclet number has been provided by for example Petrie (1999), regarding particles suspended in a fluid, as

$$Pe = \frac{G}{D_r}, \tag{2.7}$$

where G is rate of strain and D_r is the rotary diffusivity that can be expressed as the Brownian diffusion coefficient according to

$$D_r = \frac{k_B T_a}{\zeta_r}, \tag{2.8}$$

where ζ_r is the rotational friction constant, k_B Boltzmann's constant and T_a absolute temperature.

Looking in more detail at the Reynolds number, viscous forces dominate when $Re \ll 1$. This leads to a simplification of the Navier-Stokes equations, where at every point in the fluid, a balance between the local pressure and the viscous forces has to be achieved. In the limit $Re \to 0$, the inertial forces are so small that they can be neglected, and the resulting equations are linear. This flow regime is known as creeping flow. There are two interesting features worth mentioning here regarding to creeping flow:

- The flow is reversible, see for example the flow around a sphere by Schlichting (1999).
- Long-range interactions, are possible for example when particles influence each other over distances larger than their size. This is observed among settling spheres.

Newtonian fluid flow can be of two distinct types–laminar or turbulent. Laminar flow is characterised by a deterministic flow-field, which can be time dependent. Due to the physics, a laminar flow can become unstable resulting in a turbulent flow. This behaviour can also be deduced from the non-linearity of the equations, where the Reynolds number is the controlling parameter. For low Reynolds numbers, laminar flows can exist but as Re increases most flows undergo transition to turbulent flow.

The following brief summary of the phenomenon of turbulence has been provided by Tritton (1988): *"each time a flow changes as a result of an instability, one's ability to predict the details of the motion is reduced. When successive instabilities have reduced the level of predictability so much that it is appropriate to describe a flow statistically, rather than in every detail, then one says that the flow is turbulent"*

Turbulence or turbulent flow, involves a wide range of scales and Kolmogorov (see Pope (2000)) presented a theory for turbulence, based on a number of hypotheses, taking into consideration the energy production range (PR), the inertial range (IR), and the dissipative range (DR) of scales, see Figure 2.1. These hypotheses states that high-Reynolds-number turbulence can be seen as locally homogenous and isotropic if energy is constantly fed into the system and that the turbulent velocity field can be seen as eddies of different sizes. The large eddies in (PR) becomes smaller and smaller until the smallest eddies dissipate in (DR). The energy cascades from large eddies to small eddies through the intermediate region and there is no energy build up at any scales. So the intermediate eddies can be characterised by their size and velocity, or length and time scale. Kolmogorov showed on dimensional grounds that these eddies

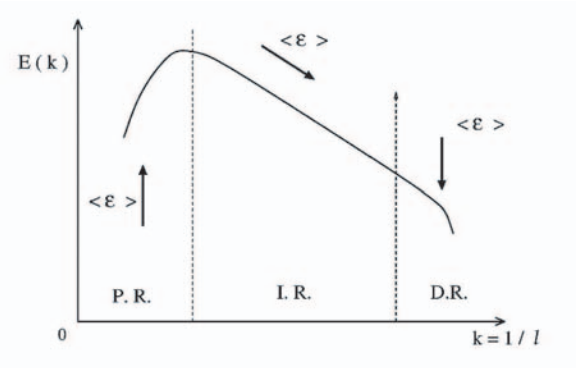

FIGURE 2.1. A schematic picture of the Kolmogorov energy cascade, from production range (P.R.), transfer in inertia range (I.R.) and finally dissipative range (DR), see *e.g.* Minier & Peirano (2001).

must be expressed in term of the energy flux ($< \epsilon >$) and the viscosity(ν). The length η and time scale τ can be shown to be

$$\eta = \Big(\frac{\nu^3}{< \epsilon >}\Big)^{1/4}, \quad \tau = \Big(\frac{\nu}{< \epsilon >}\Big)^{1/2}. \tag{2.9}$$

In order to obtain statistical quantities for the flow, the pressure and velocity are written as

$$\mathbf{U}(\mathbf{r}) + \mathbf{u}(\mathbf{r}, t) \qquad \text{and} \qquad \mathbf{P}(\mathbf{r}) + \mathbf{p}(\mathbf{r}, t),$$

where $\mathbf{r} = r_x\mathbf{e}_x + r_y\mathbf{e}_y + r_z\mathbf{e}_x$ is the spatial vector $\mathbf{U}(\mathbf{r}) = U\mathbf{e}_x + V\mathbf{e}_y + W\mathbf{e}_z$ and $\mathbf{P}(\mathbf{r})$ represent mean quantities, and $\mathbf{u}(\mathbf{r}, t) = u\mathbf{e}_x + v\mathbf{e}_y + we_z$ and $\mathbf{p}(\mathbf{r}, t)$ represent fluctuating quantities, which have a mean value that is identically zero. This decomposition is usually referred to as Reynolds decomposition and the resulting momentum equations are

$$\begin{aligned}\frac{\partial U}{\partial t} + U\frac{\partial U}{\partial x} + V\frac{\partial U}{\partial y} + W\frac{\partial U}{\partial z} = \\ -\frac{\partial P}{\partial x} + \nu\left(\frac{\partial^2 U}{\partial x^2} + \frac{\partial^2 U}{\partial y^2} + \frac{\partial^2 U}{\partial z^2}\right) - \left(\frac{\partial \overline{u^2}}{\partial x} + \frac{\partial \overline{uv}}{\partial y} + \frac{\partial \overline{uw}}{\partial z}\right)\end{aligned} \tag{2.10}$$

$$\begin{aligned}\frac{\partial V}{\partial t} + U\frac{\partial V}{\partial x} + V\frac{\partial V}{\partial y} + W\frac{\partial V}{\partial z} = \\ -\frac{\partial P}{\partial y} + \nu\left(\frac{\partial^2 V}{\partial x^2} + \frac{\partial^2 V}{\partial y^2} + \frac{\partial^2 V}{\partial z^2}\right) - \left(\frac{\partial \overline{uv}}{\partial x} + \frac{\partial \overline{v^2}}{\partial y} + \frac{\partial \overline{vw}}{\partial z}\right)\end{aligned} \tag{2.11}$$

$$\frac{\partial W}{\partial t} + U\frac{\partial W}{\partial x} + V\frac{\partial W}{\partial y} + W\frac{\partial W}{\partial z} = \\ -\frac{\partial P}{\partial z} + \nu\left(\frac{\partial^2 W}{\partial x^2} + \frac{\partial^2 W}{\partial y^2} + \frac{\partial^2 W}{\partial z^2}\right) - \left(\frac{\partial \overline{uw}}{\partial x} + \frac{\partial \overline{vw}}{\partial y} + \frac{\partial \overline{w^2}}{\partial z}\right). \quad (2.12)$$

The continuity equation becomes

$$\frac{\partial U}{\partial x} + \frac{\partial U}{\partial y} + \frac{\partial U}{\partial z} = 0, \quad (2.13)$$

where bar $\overline{f}$ represents the time average of quantity f. The resulting Reynolds equations are similar to the Navier-Stokes equations, with one significant difference; there are velocity covariances ($\overline{u^2}$, $\overline{uv}$ and so on), known as the Reynolds stresses. For general three-dimensional flow, there are now four independent equations, being the three components of the Reynolds equation and the continuity equation. However, there are $4 + 9 = 13$ unknowns. There is consequently a closure problem; commonly solved by replacing the Reynolds stress terms with model terms, such as in turbulence modelling.

The simplest way to close the equations is to use the eddy viscosity hypothesis (see for example Pope (2000)) and assume that the turbulence is isotropic. Hence, all Reynolds stress components are identical and assumed to be given by a constant multiplied with the local mean shear. There are more complete and exact ways to model the Reynolds stress term. It is also possible to solve the Navier-Stokes equations directly through direct numerical simulation (DNS) with no empirical closure models. These simulations resolve all turbulent scales and result in the time-dependent velocity at any point in the flow. However due to its high demand on computational resources, this approach is limited to low-Reynolds-number turbulence in simple geometries.

2.1. Two-phase flow

The effects of particles in a carrier phase–like spheres in a liquid–are similar to the effects of a grid or screen in turbulent flow, where turbulence is generated or attenuated depending on the grid size and turbulence intensity. Given the particle size, concentration and the initial turbulence level, turbulence is either suppressed or enhanced in two-phase flow (see for example Minier & Peirano (2001) or the experimental study by Matas *et al.* (2003)).

In general, small particles tend to suppress the turbulence level, whereas large particles seem to enhance it. This turbulence modulation can influence the carrier phase in several ways, for example leading to: displacement of the flow field by flow around the particles; generation of wakes behind the particles; modification of velocity profiles in the flow field and a corresponding change in turbulence generation; introduction of additional length scales that may influence the turbulence dissipation; transferral of turbulence energy to the motion of the dispersed phase or disturbance of flow due to particle-to-particle interactions.

As the particle generally do not follow the fluid (referred to as *the crossing trajectory effect*, see for example Crowe *et al.* (1998)), their dispersion does not equal that of the fluid. To classify particle dispersion, the Stokes number (St) is used to assess the particle behaviour in relation to the instantaneous flow motion and defined as

$$St = \frac{\tau_p U}{L}, \tag{2.14}$$

where τ_p is the time required for a particle to respond to a change in the fluid, which has characteristic velocity and length scales U and L respectively. If $St \ll 1$, the response time of a particle is faster than the characteristic time of the flow field. Hence, the particle and the fluid velocities are in velocity equilibrium, *i.e.* the particle will follow the flow. If $St \gg 1$, the particle will not respond to the fluid velocity changes, which results in a lag between the fluid velocity and particle velocity.

It is also important to consider how the fluid behaves under deformation, which can be described by a constitutive equation. This equation describes the relation between the stress in the fluid and the rate of strain, and defines the rheology of the fluid. If the stress is linearly related to the rate of strain (a linear constitutive model), the fluid is classified as a Newtonian fluid (as discussed above); in all other cases it is classified as non-Newtonian. This is the case in many flows *e.g.* polymer flows. In two-phase flows, these may be non-Newtonian, however this depends on several aspects and one is the volume concentration. For example if the volume concentration of particles in the fluid is moderate, a simplification of a Newtonian fluid (for both phases), can be used under some circumstances as long as the continuum assumption is valid.

Two-phase flows in which one phase is distributed in the other phase without mechanical connection, *e.g.* particles, are called disperse. Particle-fluid interactions are responsible for the exchange of quantities between the phases (also called coupling) for example the transfer of mass, momentum and energy between the phases. The included terms are highly specific to each flow case; for example dependent on phase character (gas, liquid or solid), chemical processes, combustion, and the degree of steadiness of the flow (for further reading see Crowe *et al.* (1998)). The coupling in two-phase flow is conceptually important here. If one phase affects the other phase with no reverse effect, this in known as one-way coupling. If there is a mutual effect between the phases, this is called two-way coupling. The latter would apply in a complete description of the two-phase flow, however the calculations present numerous challenges. Consequently, one-way coupling is most frequently used, see for example the two-phase calculations by Minier & Peirano (2001).

If the focus is restricted to solids in liquids, then a dilute dispersed two-phase flow is one in which the particle motion is controlled by fluid forces such as drag and lift. On the other hand, in a dense flow the particle motion is controlled by collisions which situation can be estimated either by considering the particle momentum response time and the time interval between collisions,

or as a mass coupling measure–the number of particles in a unit volume and the probability of collisions.

The forces acting on the particle are subdivided into: (a) body forces, such as gravity or electrostatic forces, and (b) surface forces, due to drag and lift forces, and result in a momentum coupling between the two phases. In general, the surface forces depend on particle shape and orientation, though also on the flow parameters such as the viscosity, Reynolds number, turbulence intensity etc. One fundamental example is Stokes flow around a non-rotating sphere falling in a liquid under the influence of gravity at low Reynolds number, for which the drag force varies linearly and inversely with Reynolds number.

CHAPTER 3

Fluid mechanics of fibre suspension flows

Basic fluid mechanics can been used to theoretically model the motion and coupling between a liquid and suspended fibres in order to get the bulk behaviour of the fibre suspension. The three necessary steps have been summarised by Petrie (1999), being: (1) modelling the motion of an individual fibre, (2) modelling the evolution of the orientation distribution of many fibres, and (3) estimating the contribution of fibres to the bulk stress, in terms of bulk flow.

Unlike spheres, the motion of a fibre depend on its orientation in the flow field, see for example Mackaplow & Shaqfeh (1998) who studied fibre motion during sedimentation. The fibre orientation is an important physical quantity and do not only refer to the rheology of fibre suspensions. This is seen in extrusion of fibre-reinforced composites and in papermaking where the mechanical properties are strongly linked to the fibre orientation. During these processes the understanding of the evolution of the fibre orientation distribution is also important. Hence, information regarding the transient and non-equilibrium effects are needed in order to understand fibre suspension behaviour.

3.1. The behaviour of single fibres in shear flows

The hydrodynamics of a single particle in a shear flow was addressed by Jeffery (1922) and the motion of a single ellipsoid in a Newtonian fluid is referred to as a Jefferey orbit. Looking at an ellipsoid in a simple shear but neglecting the Brownian motion of the particle–that is the tendency for a particle to assume a random distribution–the important motion is its rotation. The inertial forces can be neglected as the particle's Reynolds number is small ($Re \ll 1$). Jeffery's theory predicts a tumbling motion of a rod-like particle, which has also been confirmed experimentally. Some early experimental studies were conducted by Mason and co-workers (Trevelyan & Mason (1951) and Mason & Manley (1957)). Unlike spheres, the motion of the rod-like particle is described in an orbit, due to its initial orientation and independent in time. Consequently in a fibre suspension (no fibre-to-fibre collisions), the stress will vary periodically and never reach a steady-state condition. Jeffery's theory gives coupled differential equations for the fibre orientation in the spherical coordinates (φ, θ) and their solution as

$$\tan\varphi = r\tan\big(\frac{\dot{\gamma}t}{r+r^{-1}} + k\big), \quad \tan\theta = \frac{Cr}{(r^2\cos^2\varphi + \sin^2\varphi)^{1/2}} \tag{3.1}$$

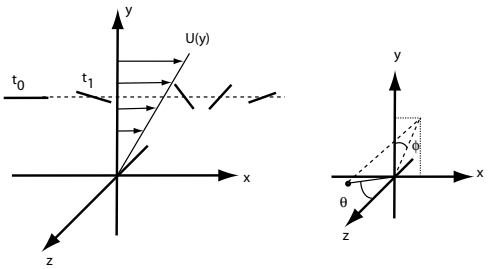

FIGURE 3.1. A simple shear flow and a single fibre under schematic rotation, where $t_0 < t_1$.

where r is the fibre aspect ratio ($r = l_p/d$ where l_p is the particle length and d the diameter), $\dot{\gamma}$ the shear rate and C and k are constants that depend on the initial orientation of the fibre.

The time t is the local time in the orbit and the constant C, can take any positive values. With C=0 the fibre is aligned along the z-axis, see Figure 3.1, and with C$\rightarrow \infty$ the fibre is rotating in the xy-plane. Thus, in order to describe the periodic fibre flipping motion in a shear flow different terms like "director tumbling", "log-rolling" and "kayaking" have been used in the literature. The pathline given by the intersection of the axis of symmetry of the particle and a unit sphere is used to describe the fibre orientation, see Figure 3.2, where Jeffery orbits for different values of C can be seen. This theoretically obtained result has also been confirmed experimentally, see *e.g.* Trevelyan & Mason (1951). Single fibre motion was further explored by Hinch & Leal (1972). They included the effect of Brownian motion in their study, which was excluded by Jeffery.

The time the fibre spends in the orbit depends on the shear rate and the aspect ratio. In general, very long, slender fibres are aligned in the flow direction most of the time, and the time spent flipping is somewhere in the order of r^{-1}. For very slender particles, fibre aspect ratio $r \gg 1$, the theory by Jeffrey can be simplified, which was presented for example by Burger (1938). The result of the simplified coupled differential equations are

$$\frac{d\theta}{dt} = \frac{\dot{\gamma}}{4} \sin 2\theta \sin 2\varphi \tag{3.2}$$

$$\frac{d\varphi}{dt} = \dot{\gamma} \cos^2 \varphi. \tag{3.3}$$

Jefferys theory inspired both theoretical and experimental studies and a relation between the rate of rotation and the aspect ratio resulted in an introduction of an effective aspect ratio. Bretherton (1962) extended the work by Jeffery and showed that any fore-and-aft symmetric particle rotates with the period

$$t_r = \frac{2\pi}{\dot{\gamma}} \left(r_e + {r_e}^{-1} \right) \tag{3.4}$$

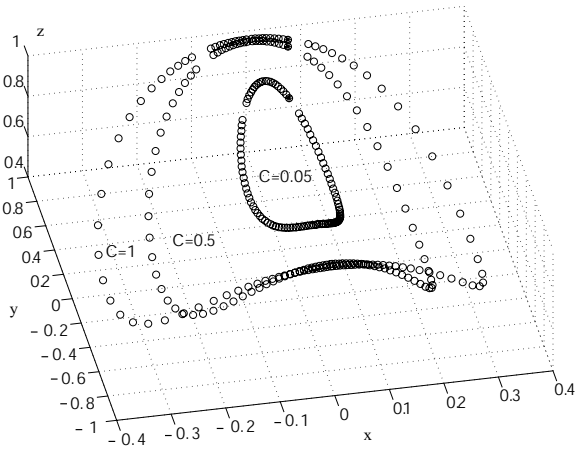

FIGURE 3.2. The Jeffery orbit for different constants of C, the pathline of the fibre end.

if an effective aspect ratio r_e is used.

However, several studies has tried to determine a uniquely defined effective aspect ratio, but this has not been realized. The values depend on the aspect ratio regime and shape of the fibre ends. Experimentally Mason & Manley (1957) estimated that $r_e = 0.7r$ for aspect ratios $r \approx 20$. Generally, the effective aspect ratio tend to be less than the actual aspect ratio, which is a results of that fibres tend to rotate faster than predicted by theory.

3.2. Influence of fibres at low concentration

Theoretical work by Cox (1970) resulted in a model of torque and forces on a solid, long, slender body in a given undisturbed Stokes flow. In his slender body theory Cox included interaction (no collisions) between two or more slender bodies as well the effect of a wall. The force and torque were derived for straight slender bodies as well as for curved slender bodies. Cox also derived a theory for the forces acting on flexible fibres and incorporated buckling, which is observed for flexible bodies in shear flow. In addition, he proposed a modification for the case of small but finite particle Reynolds number. For this case, the inertia effects resulted in a modification to the orbit constant C, given by the theory by Jeffery. Cox applied the model on a shear flow and the result was a rheological behaviour of the suspension in an efficient viscosity.

Contemporary to Cox's work Batchelor (1970*b*) presented a theoretical model for slender bodies and the contribution to bulk stress. The bulk stress related to the instantaneous particle orientation, averaged over an ambient fluid volume and a number of particles (m), is given by

$$\sum{}_{ij}^{(m)} = \frac{1}{V} \sum \int_{A_0} \sigma_{ik} x_j p_k dA \tag{3.5}$$

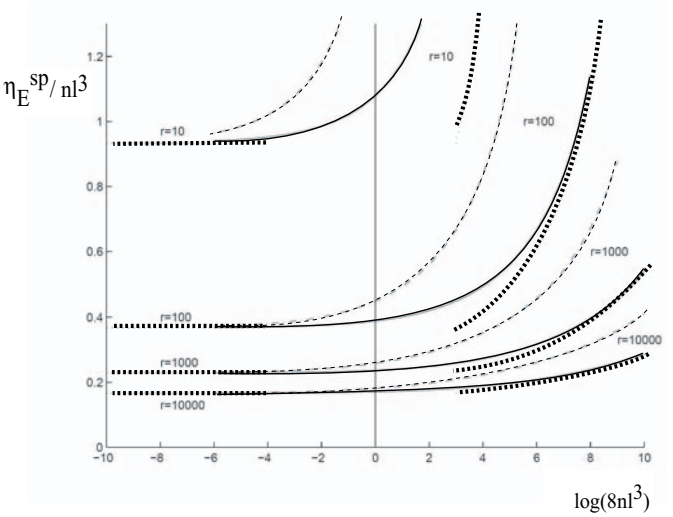

FIGURE 3.3. The specific viscosity as a function of concentration for different aspect ratios r, the dashed lines represent the theory of Batchelor and the solid lines represent the interpolation formula presented by Petrie (1999).

where the integral is taken over the particle surface A_0 and the summation is over the particles in volume V. The force exerted on the particle surface by the ambient fluid at a point where the unit normal is $\mathbf{p}$, is given by $\sigma_{ik}p_k$.

By applying this Batchelor (1971) presented an theoretical estimate of the change in extensional viscosity. In dilute suspensions, *i.e.* particles do not interact, the fractional increase in bulk stress due to presence of the particles is equal to the volume concentration times l_p^2/b^2, where l_p is the particle length and $2b$ is the cross-sectional size. Batchelor concluded that the stress due to particles may be relatively large for very dilute suspensions and that particle length has a dominant influence on the extensional viscosity. His work was extended to particles of arbitrary shape in Batchelor (1970*a*) and for semi-dilute suspensions in Batchelor (1971).

In Figure 3.3 an example is plotted. The specific extensional viscosity is divided by the volume concentration, expressed in term nl_p^3, against the logarithm of the concentration. The extensional viscosity is shown for different aspect ratios, r. The dotted line shows the theory of Batchelor and the solid line is an interpolation taken from Petrie (1999) (dashed line is the limiting line suggested by Petrie), which connects the effect for a dilute suspension to the semi-dilute suspensions regime. Hence, this is an extension to the work by Batchelor. The dilute suspensions refers to $nl_p^3 \ll 1$ which can be visualised as a unit volume that contains the number n fibres.

3.3. Non-dilute fibre suspensions

According to e.g.Petrie (1999) the criteria for a dilute suspension is $c_v \ll r^{-2}$, where c_v is the volume concentration. The semi-dilute range is given by $r^{-2} \ll c_v \ll r^{-1}$ and $c_v \gg r^{-1}$ thus implies a concentrated suspension. In the work by Dinh & Armstrong (1984), Batchelor's work was modified to include the presence of non-dilute suspensions. They presented, for small strain in simple shear flow, a result for the specific viscosity

$$\eta^{sp} = \frac{\pi n {l_p}^3}{90 \log(h/l_p)}, \tag{3.6}$$

where n is the number density of the fibres with a fibre length l_p and a mean spacing between the fibres h. In the case of uniaxial extension flow the equivalent specific viscosity is given by

$$\eta_E^{sp} = \frac{\pi n {l_p}^3}{30 \log(h/R_p)}, \tag{3.7}$$

where $R_p = d_p/2$ is the fibre radius. A deeper physical interpretation of effective elongational viscosity of non-dilute suspension of aligned slender bodies is given in Acrivos & Shaqfeh (1988).

Comprehensive work in the area of semi-dilute suspensions has been done by Shaqfeh & Fredrickson (1990), who presented a "multiple scattering" approach to model the effects of many fibres. This approach gives a rigorous derivation of stress for an arbitrary orientation distribution in a semi-dilute suspension. A length is introduced associated with the transition between the near-field of the fibres, which consist of the pure suspending fluid, and the far-field and interaction with other fibres. They derived a value for this length for different flows, not only aligned flows as Doi & Edwards (1986), and there are some similarities with this work and the cell size introduced by Batchelor (1971). However, the complexity of the models increase when one leaves the dilute regime. The slender-body theory extends into the semi-dilute regime but can not describe concentrated suspensions.

One important aspect of fibre suspension flow is colliding effects and fibre-fibre interaction, as pointed out by Folgar & Tucker (1984). Their approach to include these effects in semi-dilute suspension, was to introduce an empirical rotary diffusion term (D_r). The rotary diffusion, see Equation 2.8, was suggested by Folgar and Tucker to be proportional to the shear rate. A number of theoretical and experiments have confirmed the basic assumptions made by Folgar & Tucker. It can be noted that this model has some similarities to the modelling of turbulence, *i.e.* the closure of the equations, the appeared constant C_r has to be determined, either on theoretical basis or *ad hoc*.

The rotary diffusivity for different flows, such as simple shear flow and extensional flow, has been calculated and measured by Anczurowski & Mason (1967) and Stover *et al.* (1992). For extensional flow, a theoretical result

was obtained by Shaqfeh & Koch (1988). This was experimentally verified by Rahnama *et al.* (1995).

For colloidal suspensions the effect of van der Waals forces, electrostatic forces as well as Brownian forces becomes important, influencing the rheology. However, from the fibre point-of-view this may be seen as a modification of the rheology of the suspending fluid although these effects can be important when direct fibre-to-fibre interaction is considered. If real suspensions should be modelled it is important to formulate a correct constitutive equations. For most cases this means that experiments are required in order to determine constants in the model. If, an appropriate model could be developed for pulp suspensions, this would be the case since the properties of different pulp fibres are vastly different.

3.4. Pulp suspensions

Fibre suspensions are an important part of many different industrial processes, *i.e.* manufacturing of fibre-reinforced composites or in papermaking. Concentration, aspect ratio and flexibility are probably the crucial parameters that should be used to classify different suspensions. In addition, the fibre orientation have a definite influence on the rheological characteristics already at low concentrations.

Fibres used in papermaking are slender particles, which are hollow and flexible varying greatly in length and diameter, dependent on the species of plant they are derived from, and the local growing conditions. Once separated from the original plant (tree) they tend to curl or kink. Pulp fibres consist typically of 40-50% cellulose, 20-35% hemi-cellulose, 15-35% lignin, and the remaining fraction contains resins, tannins, ash and a whole range of miscellaneous compounds, see for example Fellers & Norman (1998).

One of the essential difficulties with papermaking fibre suspensions is that under typical processing conditions these fibres tend to aggregate into "flocs" or "clumps", see for example the review by Kerekes *et al.* (1985). Although flocculation may occur by surface charges, Mason & Manley (1957) found that mechanical entanglement rather than colloidal forces was the principle reason for flocculation. They entangle, bend, and remain networked from frictional forces transmitted by fibres that are locked into bent configurations. It is well established that fibre flocs is generated by mechanical entanglement.

Experimental observations of pulp suspension have been carried out during the years and in some early work the effect of shear and wall effects, on a pulp suspension were studied by Steenberg & Wahren (1961). In addition, they observed concentration gradients close the wall. Fibre-segment disruption has been experimentally presented by Steenberg *et al.* (1961). In a study by Andersson (1966) showing the effect of flocculation in pulp suspensions.

In a numerical study by Steen (1991) of flocculation in turbulent flows, a measure for the rate of rupture and aggregation in pipe flow and backward facing step flow was introduced. Shear flow is one flow condition in where this

is obtained but extensional flow is shown to be more efficient in dispersing fibre flocs. This was first demonstrated by Kao & Mason (1975) and experimentally verified by Norman & Duffy (1977). Studies of floc rupture in shear flow has also been made by Lee & Brodkey (1987) and flow rupture in extensional flow was studied by James *et al.* (2003). In a work by Blaser (2000) the mechanism of shear and strain on floc motion was presented but not for pulp suspensions. However, the observations are similar to what has been reported for pulp suspension flows.

Soszynski & Kerekes (1988) confirmed the influence of bending stresses on floc strength through stress relaxation experiments. They defined the propensity for paper-making fibres to flocculate in terms of a dimensionless number, termed the crowding number N

$$N = \frac{2}{3} c_v r^2 \tag{3.8}$$

where c_v is the volume fraction of the solid material in the suspension, and r is the fibre aspect ratio. The physical significance of N can be seen in its definition: N reflects the number of fibres in a spherical volume of diameter equal to unity. This definition can be related to the more widely used measure of particle concentration–the number of particles per unit volume (n) through $n = 6N/(\pi l_p^3)$. Flocculation does not generally occur when $N \ll 1$, as each fibre can rotate freely. In the range $1 < N < 60$, fibres flocculate in simple shear flow see *e.g.* Soszynski & Kerekes (1988). It is in this range that most papermaking processes operate. Fibre mobility is greatly hindered when $N > 60$, as the suspension forms networks, with each fibre making contact with on average three other closely located fibres, see Meyer & Wahren (1964). The crowding number was supplemented by a fibre Reynolds number and a force factor in an overview by Kerekes (1995). The use of a crowding number has been further extended by Kiviranta & Dodson (1995) in characterising the mix conditions during paper forming.

As previously mentioned, the rheologies of pulp suspensions are complex though important, since the interaction of the fibre suspension and the flow field results in some very specific characteristics (see Niskanan *et al.* (1998) and Björkman (1999)). In pipe flows at low flow velocities, pulp suspensions will flow like plug flows. Plug flows characteristically flow has an almost homogenous velocity profile is obtained through most of the pipe and close to the wall a thin lubricating water layer is observable. As the velocity increases, the shear at the wall will cause rupturing at the individual fibre level or at the forming floc level, or both. This is referred to as turbulence in some cases, however there is a suggestion that it ought to be called fluidised flow (see Söderberg (1999)). As the velocity increases further, the centre plug flow gradually breaks up and becomes fluidised.

In turbulence in a Newtonian fluid, the continuous spectrum of scales are most probably influenced by the presence of fibres in the flow. The small eddies, in order of the fibre size, are presumably suppressed and the larger eddies are

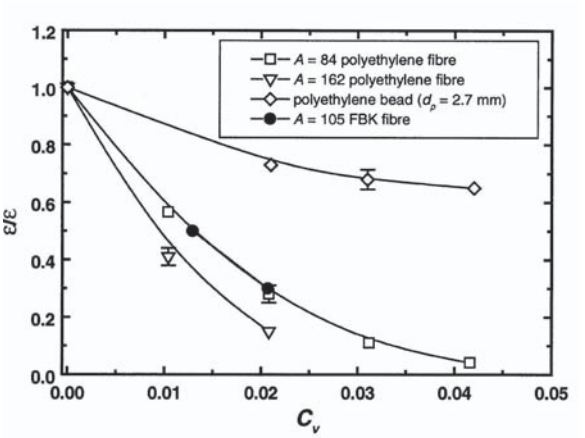

FIGURE 3.4. Relative liquid-phase energy dissipation versus volumetric concentration for fibres of different aspect ratios, A, and for a suspension of polyethylene beads. Result for fibre suspensions with polyethylene fibres or kraft fibre suspension (FBK) are shown in the study by Bennington & Mmbaga (2001).

influenced due to flocs and in overall this changes the turbulent spectrum. The dissipation of kinetic energy is changed, since energy is transferred from large scales to the fibre network. This turbulent modification was indicated in the study by Ljus *et al.* (2002) and also by Matas *et al.* (2003). In an experimental study by Bennington & Mmbaga (2001), a reactive chemical was used in a pulp suspension of 4% and this indicated that 95% of the energy dissipation was transferred to direct fibre friction and only 5% of the energy dissipated in the fluid itself (see Figure 3.4). This experiment indicates that modification to a non-continuous spectrum by increasing the concentration of fibres leads to non-linear effects. This can be evidently be seen as an increase in the viscosity. In a study by Ralambotiana *et al.* (1997), the increase of viscosity due to changing the fibre aspect ratio and the concentration was studied, and revealed that this could be significant, with an increase in viscosity in the vicinity of 20-30%, even for very low concentrations.

Recently, there has been extensive simulations by Klingenberg and his co-workers regarding fibre suspension of higher concentration, where entanglement and network of fibres are expected. A model and technique for entangled fibres and fibre network, flocs, is presented in Schmid *et al.* (2000). The flexibility of the fibres are simulated in segments with forces and torque in the segment joints.

In the study by Stockie & Green (1998) an approach of using a immersed boundary method in order to simulate the motion of flexible pulp fibres. This

motion was calculated in a two-dimensional shear flow at moderate Reynolds number. A very recent work by Tornberg & Shelly (2004) numerically studied the dynamics of flexible fibres in Stokes flow. Tornberg and Shelly used a non-local slender body theory and could obtain shear induced buckling and relaxation of the filaments, leading to an elastic energy concepts, which is very unique for a fibre suspension compared to suspension of spherical particles.

In general, these effects are implicit in non-Newtonian suspensions, however in pulp suspensions at low concentrations, viscosity may be simplified to being constant and thus independent of the flow field. This implied that the suspension can be treated as Newtonian as a first approximation. Simulations involving modelling of pulp suspensions are in their initial stage, however extensive experimental studies of pulp suspensions have been undertaken in parallel with the development of papermaking machines.

CHAPTER 4

Summary of the papers

Paper 1

The first paper summarizes the pressure and wire position measurements performed in an experimental facility called the KTH-Former. The KTH-Former intends to model mechanisms in the roll forming zone of a paper machine. It includes a headbox, a roll and a wire, which can reproduce a one-sided dewatering event. Measurements were carried out with pure water for three different wires: non-permeable, semi-permeable and conventional open wire. Although not useful in papermaking, the non-permeable wire is relevant when trying to understand the mechanisms of roll forming. In the study, the pressure profile and the distance between the solid roll and the wire was measured along the wrap angle on the roll. The wrap angle is measured from the position were the free-jet from the headbox impinges on the wire to the point where the wire separates from the roll, Figure 4.1. Depending on the wrap angle the forming roll can result in partial or complete roll dewatering. For the case of partial dewatering the web is still saturated at the point where it separates from the roll. The measured pressure distribution showed a more complex pattern than the simple model $p = T/R$, which normally is referred to as the nominal pressure (T is wire tension and R roll radius). An example of an obtained pressure distribution for the non-permeable wire is shown in Figure 4.3.

It is shown that an increase in wire tension has a similar effect as a decrease in flow-rate (jet flow rate from the headbox) on the shape of the pressure distribution. This is a consequence of that the flow to a large extent is governed by the relation between the dynamic pressure and the nominal pressure. For the case of partial dewatering the suction peak that appears at the roll-wire separation point has a strong influence on the pressure distribution upstream. Finally, it is shown that the drainage has a stabilizing effect on the dewatering pressure.

Paper 2

This paper formulates a physical model that is intended to explain fundamental mechanisms that control partial dewatering in roll forming in papermaking. The flow around the forming roll is modelled in a cylindrical coordinate system and the wire is assumed to be impermeable. The governing equations are reduced based on a discussion where the magnitude of the different terms is

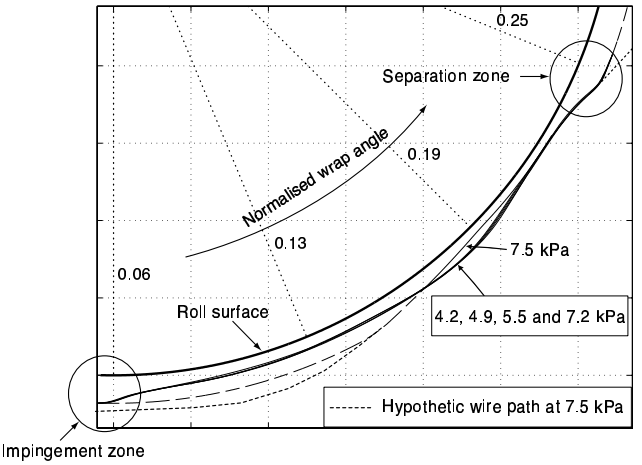

FIGURE 4.1. Wire position as function of normalized wrap angle for five different nominal pressures $p = T/R$. The dashed line corresponds to the outer measurement range of the position transducer and the dotted line corresponds to a possible wire path for the 7.5 kPa case.

estimated. Given this reduced set of equations a non-linear equation for the position of the wire is deduced.

This equation clearly shows that one of the most important parameters is the Weber number, *We*, which is the non-dimensional number that can be obtained by comparing the effect of wire tension (surface tension) in relation to the momentum of the incoming headbox jet.

The non-linear equation is linearized around the trivial solution to the equations, which gives that the wire is displaced a constant distance from the roll along the whole wrap length. The linear equation is shown to have a standing wave solution that gives a specific wavelength. This solution is compared to previously measured data (see *Paper 1*) regarding the wavelength of the waves and showed in Figure 4.3

Clearly the permeability of the wires (and the fibre mats formed at the wires) has a strong influence on the flow in the roll-forming zone of a paper machine. However, the experimental results obtained in *Paper 1* show that standing waves also are present with a permeable wire. Hence, given a specific forming situation there will probably be a threshold value for the Weber number. On one side of this value the process will be stable and on the other side waves will appear.

The result pinpoints the importance of the Weber number, which also can be of importance on a day-to-day basis in a modern paper mill.

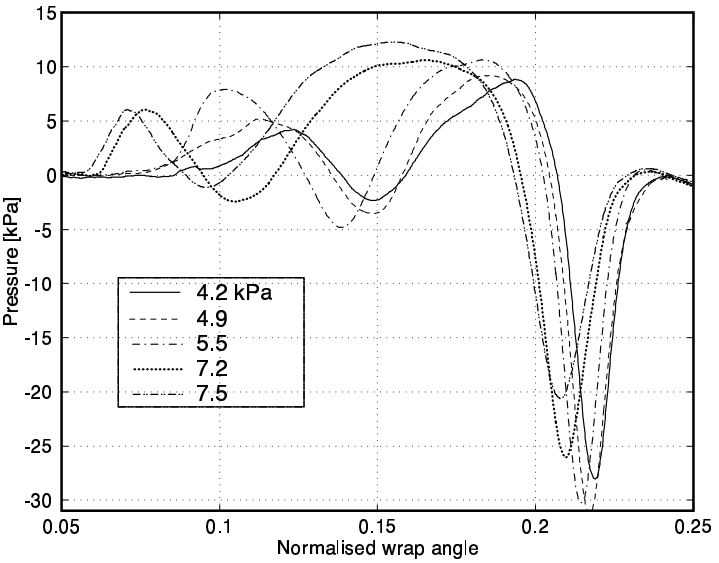

FIGURE 4.2. The measured pressure distributions at the roll surface with the non-permeable wire for different nominal pressures (changed the wire tension T).

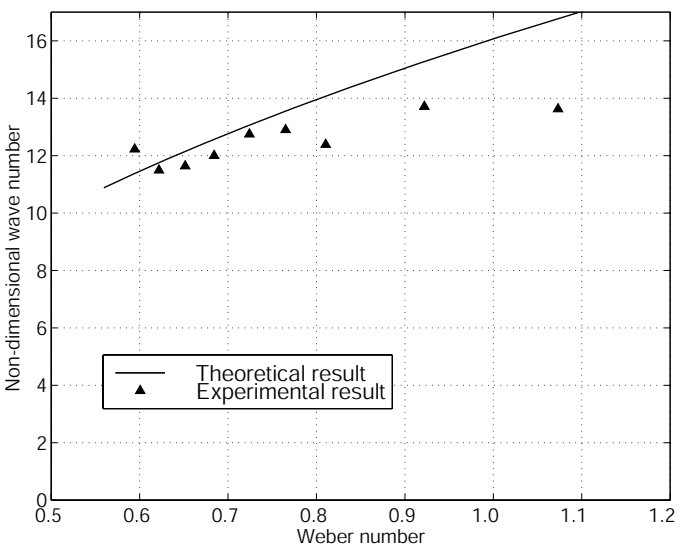

FIGURE 4.3. Normalised wave number to Weber number, *We*, for the case of non-permeable wire. Experimental result refer to data obtained in *Paper 1*.

Paper 3

In this study the sedimentation of rigid fibres at a finite but small Reynolds number has been studied. Understanding of the settling motion of dilute fibre suspensions is difficult as each individual fibre moves under the influence of the long-range hydrodynamic disturbances of the other fibres. Insight into this phenomena can be gained by first examining the simplest case of the motion of a single isolated fibre settling under Stokes' flow conditions.

Unlike spheres, isolated fibres can have significant motion perpendicular to gravity with a drift velocity strongly dependent upon its orientation. With swarms of settling fibres this situation becomes more complex as each individual fibre moves under the influence of the long-range hydrodynamic disturbances of the other particles. These forces tend to affect the motion of the neighboring particles and lead to inhomogeneous settling rates.

As shown in Figure 4.4, two distinct settling behaviours were observed. The settling velocity of these fibres display somewhat similar behaviour as that reported by Herzhaft & Guazzelli (1999) and by Herzhaft *et al.* (1996), *i.e.* non-monotonic for small volume concentration. We did observe individual fibres, however, with velocities approximately four-times that of the isolated fibre. In addition we observed the trajectories of the fibres and classified the observed motion into three groups: simple downward or upward motion with drift; recirculating or meandering motion; or groups of fibres with correlated motion. We observed fibres with correlated motion over length scales greater that $2l_p$ (l_p is fibre length). We interpreted this as evidence of particle clumping.

In the semi-dilute regime, fibres recirculated in swirls which appeared as eddy-like structures of size $\approx 15 - 20\, l_p$, see Figure 4.5. Over the concentration ranges tested, we characterized the velocity fluctuations as the standard deviation σ of the histogram and find that both the drift and settling fluctuations are proportional to $\phi^{1/3}$, similar to the findings reported Segre *et al.* (1997) for settling spheres.

Paper 4

The purpose of this experimental work was to study the wall effect, or influence of shear, on fibre orientation in suspensions with different fibre aspect ratios and concentrations. We have studied a suspension flow on an inclined plate. The fibre orientation at different wall parallel planes were measured.

We have applied an index-of-refraction (IR) matching method to gain optical access into the fibre suspension. IR-matching was used together with particle tracking techniques and the fibre orientation was extracted using a two-dimensional wavelet transform using LabView.

For low concentration (nL^3=0.009 and nL^3=0.09) and low aspect ratio (r=10) fibres are oriented perpendicular to the streamwise direction in the near wall region, see an representative result in Figure 6.

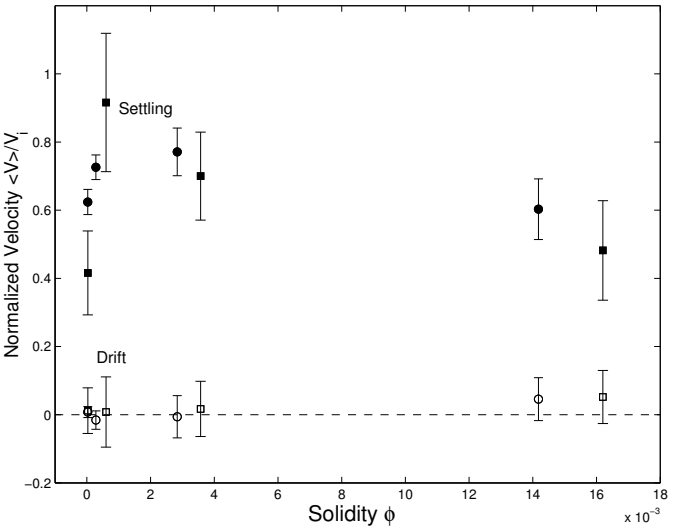

FIGURE 4.4. The normalized average settling and horizontal drift velocities as a function of volume concentration ϕ for aspect ratios $r = 23$ ($\circ$) and $r = 50$ ($\square$). The settling velocity is defined by $V_{\parallel}$ and the drift velocity by $V_{\perp}$. The uncertainty in the data is represented the standard error of the mean estimated at the 95% confidence interval.

An increase in fibre concentrations result in increased hydrodynamic interactions in the fibre suspension. However, the present results show an effect on fibre orientation for twice the distance into the suspension compared to what has previously been reported (see for example Russel *et al.* (1977)). The influence was observed as a wider fibre orientation distribution and as a shift in the maximum fibre orientation.

Paper 5

A technique of ultrasound to measure fluid velocity non-intrusively in opaque fluids has been tested and evaluated. The ultimate goal, of which the present work provides the first steps, is to measure turbulent flow properties in cellulose fibre suspensions. The idea is is to determine the velocity of the flow from ultrasound echoes reflected by particles in the fluid, see Figure 8.

A commercial Ultra Velocity Profiler unit, which determines the velocity based on the doppler shift of the ultrasound frequency is tested. The commercial unit is found to be suitable for measurements of mean properties. However, the spatial and/or temporal resolution of the measurements is limited. The unit is thus not suitable for measurements of turbulent velocity fluctuations. These limitations might be surmountable by alternative signal processing. A number

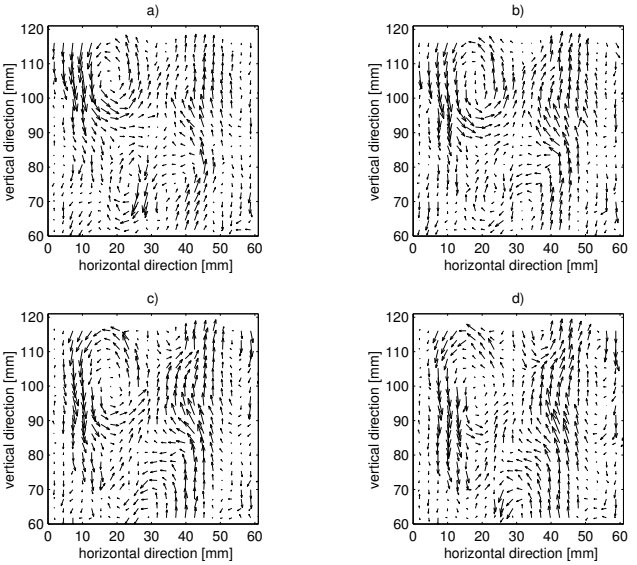

FIGURE 4.5. PIV results on fibre aspect ratio $r = 23$ suspension at volume concentration $\phi = 1.4 \times 10^{-2}$ sampled at the midplane in the sedimentation cell. Four different times are shown (a) $16.5s$ (b) $16.9s$ (c) $17.3s$ and (d) $17.7s$. The image can be scaled using $1.4mm \mapsto 1mm/s$.

of methods are proposed and some are evaluated. It is believed that ultrasound based methods will be useful in the characterisation of turbulent flow in fibre suspensions.

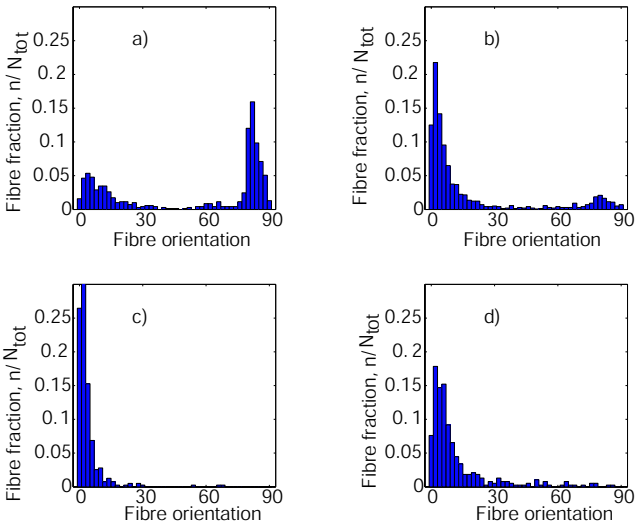

FIGURE 4.6. The fibre orientation distributions for $r = 10$ and concentration nL^3=0.009 for different wall parallel plans, a) $z = 1 \pm 1\,mm$ b) $z = 3 \pm 1\,mm$, c) $z = 6 \pm 1\,mm$ and d) $z = 9 \pm 1\,mm$.

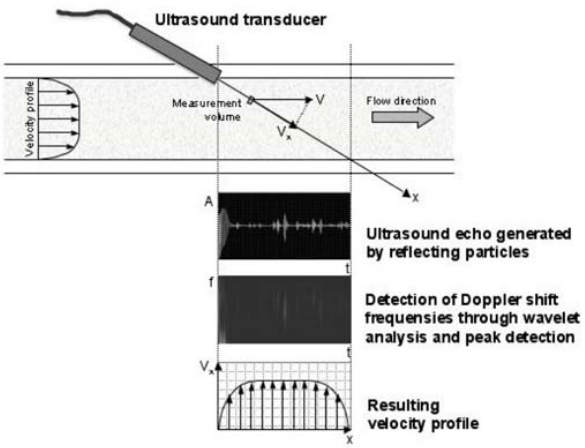

FIGURE 4.7. Ultrasonic velocity measurement by determining the Doppler shift from the wavelet transform.

CHAPTER 5

Papers and authors contributions

The scientific papers and the authors contribution as well as where the results have been presented.

Paper 1. Holm R., Söderberg D. & Norman B., 2004 Experimental studies on the partial dewatering during roll forming of paper, to appear in *Nordic Pulp and Paper Research J.*

RH has designed the experiment based on discussions with the co-authors (DS, BN). RH has carried out the experiments and evaluated the data. RH has together with the co-authors prepared the paper. In addition, Prof. P.H.Alfredsson, KTH Mechanics has contributed to all parts of the work.

Paper 2. Holm R., & Söderberg D., 2004 A theoretical analysis of the flow stability in roll forming of paper, to appear in *Nordic Pulp and Paper Research J.*

The theoretical analysis, the evaluation of the results and preparation of the paper has been perfomed by RH together with DS. Data for these two paper has its origin from the licentiate thesis of RH, Holm (2002). Part of the results has been presented at PAPTAC, 89^{th} Annual Meeting PAPTAC 2003, Montreal, Canada.

Paper 3. Holm R., Storey, S., Martinez M., & Söderberg D. 2004, Visualization of streaming-like structures during settling of dilute and semi-dilute rigid fibre suspensions, submitted to *Physics of Fluids*

RH has performed the experiments in collaboration with SS under the supervision of MM. RH carried out the PIV-measurements and the post-processing of the data. The data evaluation algorithm was developed by DS and modified by RH. The paper was written by RH, primarily together with MM. The experiments were conducted at University of British Columbia, Vancouver, Canada. Part of the results was presented at the Paper Physics seminar, 2004 in Trondheim, Norway.

Paper 4. Holm R. & Söderberg D. 2004 Influence of shear on fibre orientation in the near wall region, to be submitted

RH has designed the experiment based on discussions with the co-author DS. RH has carried out the measurement and evaluated the data. The data evaluation algorithm was developed by DS and modified by RH. RH has together with DS prepared the paper.

Paper 5. Fällman M., Holm R., Lundell F. & Söderberg D. 2004 The use of ultrasonic measurement in suspensions, STFI-Packforsk report, PUB 20, 2004.

RH has designed the experiment together with DS and RH participated in the development of a modified UVP-technique together with MF and FL. RH has participated in the analysis of the technique and supported MF and FL in the preparation of the paper.

APPENDIX A

Single-sided roll forming

The experimental findings of the pressure profile, wire position and the expelled amount of water are shown in Figure A.1. These measurements were conducted in partial dewatering in single-side roll forming, with a semi-permeable wire and water to simulate the mechanism of web build up in paper making. The measurements with the saveall was a time consuming procedure, during which the system was challenged when keeping a constant flow of 400 l/min in the KTH-Former. The mean drainage rate (over $\hat{\varphi}$=0.005) is shown together with the corresponding pressure and wire position for the semi-permeable case at a nominal pressure of 5.9 kPa. From the figure, it is clearly seen that the amount of expelled water agrees well with the pressure profile, with two significant peaks and a minimum around $\hat{\varphi}$=0.12. Even if there are experimental challenges to adjust the saveall to get sufficiently close to the wire to collect the expelled water without touching the wire. The result from the saveall measurements showed that approximately 30 % of the total flow was drained within the dewatering zone. This means that a substantial amount of the water passes through the dewatering zone, so this case can indeed be described as partial dewatering.

One way of checking the consistency of the experimental data is to integrate the pressure data to determine the corresponding wire positions. The relation between the pressure and the position is given by equation (A.1).

$$p_{wire} = T\big[\frac{1}{R} - g''(s)\big], \tag{A.1}$$

where T is the wire tension [N/m], R is the roll radius [m] and g(s) is the distance between the roll surface and the position of the wire along the coordinate s, $s = \varphi R$.

The results from such integrations are shown in Figure A.2 where the measured wire position and the calculated position based on the pressure data are shown. The calculated positions show good agreement with the measured ones. However, the calculated data points starts to deviate from the measured ones if the position of the second boundary condition is chosen downstream of the inflection point in the wire positions (at $\hat{\varphi} \approx 0.17$). The upstream point for

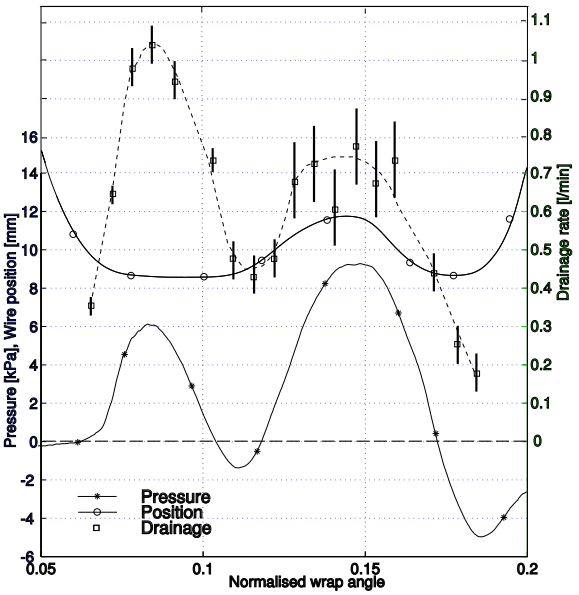

FIGURE A.1. The measured pressure and wire position with the corresponding drainage rate, average data from figure **??**.

the calculation was chosen at $\hat{\varphi}$=0.076. The deviation of the calculated position is obvious when chosen the second boundary condition at $\hat{\varphi} \approx 0.19$. We interpreted this as evidence of strong affect on the forming event due to the roll-wire separation.

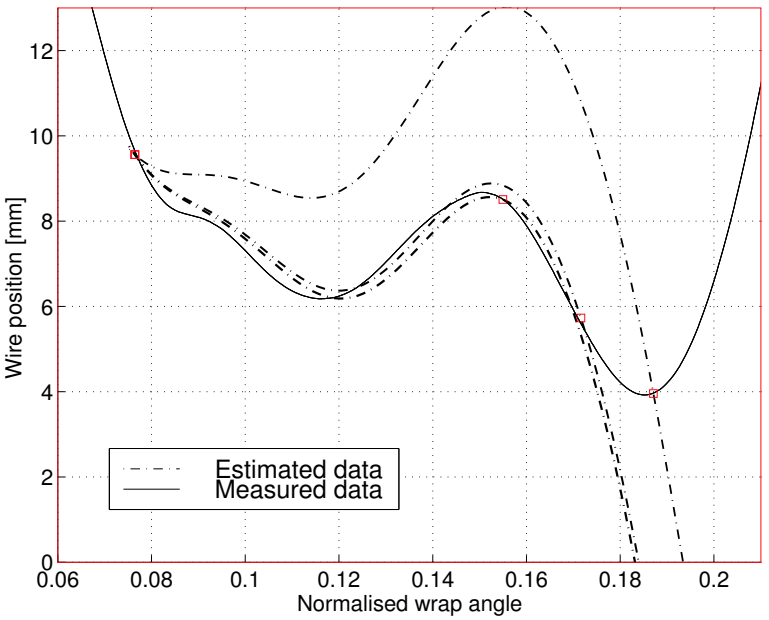

FIGURE A.2. Measured wire position and calculated position of the wire based on pressure data. Data obtained at nominal pressure 4.5 kPa and non-permeable wire

Bibliography

Acrivos, A. & Shaqfeh, E. S. G. 1988 The effective thermal conductivity and elongational viscosity of a non-dilute suspension of aligned slender rods. *Phys. Fluids.* **31**, 1841–1844.

Anczurowski, E. & Mason, S. G. 1967 The kinetics of flowing dispersions iii. equilibrium orientations of rods and discs (experimental). *J. Colloid Int. Sci.* **23**, 533–546.

Andersson, O. 1966 Some observation on fibre suspensions in turbulent motion. *Svensk Papperstidn.* **69** (2), 23–31.

Bandhakavi, V. & Aidun, C. 1999 Analysis of turbulent flow in the converging zone of a headbox. In *Tappi Engineering Conference, Annaheim*, pp. 1135–1154.

Batchelor, G. K. 1970*a* Slender-body theory for particles if arbitrary cross-section in stokes flow. *J. Fluid Mech.* **44** (3), 419–440.

Batchelor, G. K. 1970*b* The stress system in a suspension of force-free particles. *J. Fluid Mech.* **41** (3), 545–570.

Batchelor, G. K. 1971 The stress generated in a non-dilute suspension of elongated particles by pure straining motion. *J. Fluid Mech.* **46** (4), 813–829.

Bennington, C. & Mmbaga, J. 2001 Liquid phase turbulence in pulp fibre suspensions. *Proc.The 12th Fundamental Research Symposium, Oxford.*

Bergström, R. 2003 Fibre flocculation during twin-wire roll forming. Lic thesis, Div. Paper Tech., Dept. Fibre and Polymer Tech., KTH, Stockholm.

Björkman, U. 1999 *Flow of flocculated fibres*. Kungl Tekniska Högskolan, avd. Pappersteknik.

Blaser, S. 2000 Flocs in shear and strain flows. *J. Colloid and Interface Sci.* **225** (-), 273–284.

Bretherton, F. P. 1962 The motion of rigid particles in a shear flow at low Reynolds number. *J. Fluid Mech.* **14**, 284–304.

Burger, J. M. 1938 *On the motion of small particles of elongated form suspended in a viscous liquid: 2nd report on viscosity and plasticity*. North-Holland Publ., Amsterdam.

Chen, E., Schultz, W. & Perkins, N. 1998 A two-dimensional viscous model of a wet paper forming process. In *Tappi Engineering Conference*, pp. 21–.

Chuang, S. 1982 Microturbulence generation in a papermachine headbox. In *Tappi Engineering Conference*, pp. 205–213.

Cox, R. G. 1970 The motion of long slender bodies in a viscous fluid, part 1 general theory. *J. Fluid Mech.* **44** (4), 791–810.

Crowe, C. T., Sommerfeldt, M. & Tsuji, Y. 1998 *Multiphase flows with droplets and particles*. CRC Press LLC.

Dalpke, B. 2002 Modelling of jet impingement and early roll forming. PhD thesis, Dept. of Mechanical engineering, University of British Colombia, Vancouver.

Dinh, S. M. & Armstrong, R. C. 1984 A rheological equation of state for semi-concentrated fibre suspension. *J. Rheol.* **28**, 207–227.

Doi, M. & Edwards, S. F. 1986 *The theory of polymer dynamics*. Oxford University Press.

Farrington, T. A. 1991 A numerical investigation of three tissue machine headboxes. In *AIChE Proceedings, Forest Products Symposium*, pp. 177–188.

Fellers, C. & Norman, B. 1998 *Pappersteknik*. Kungl Tekniska Högskolan, avd. Pappersteknik.

Folgar, F. & Tucker, C. L. 1984 Orientation behavior of fibres in concentrated suspensions. *J. Rheinf. Plast. Composites* **3**, 98–119.

Gooding, R., McDonald, D. & Rompr, A. 2001 Measurement of drainage around a forming roll. In *87th Annual Meeting, PAPTAC, Monteral*, pp. A125–138.

Herzhaft, B. & Guazzelli, E. 1999 Experimental study of the sedimentation of dilute and semi-dilute suspensions of fibres. *J. Fluid Mech.* **348** (-), 133–158.

Herzhaft, B., Guazzelli, E., Mackaplow, M. B. & Shaqfeh, E. S. G. 1996 Experimental investigation of the sedimentation of dilute fibre suspensions. *Phys. Rev. Lett.* **77** (2), 290–293.

Hinch, E. J. & Leal, L. P. 1972 The effect of Brownian motion on the rheology properties of a suspension of non-spherical particles. *J. Fluid Mech.* **52**, 683–712.

Holm, R. 2002 On the fluid mechanics of partial dewatering during roll forming in paper making Lic thesis, Dept. of Mech., Royal Institute of Technology (KTH), Stockholm, Sweden.

Holmqvist, C. 2002 Modelling of the pressure distribution in twin-wire blade formers Lic thesis, Dept. of Mech., Royal Institute of Technology (KTH), Stockholm, Sweden.

Hua, L. & et. al 1999 A numerical investigation of three tissue machine headboxes. In *Tappi Engineering Conference, Annaheim*, pp. 1123–1133.

Hyensjö, M., Krochak, P., J.Olson, Hämäläinen, J. & Dahlkind, A. 2004 Modelling a turbulent dilute fibre suspension in a planar contraction: Effect of vane types, vane position and wall boundary layer on fibre orientation distribution. In *5th International Conference on Multiphase Flow, ICMF04*, p. 436.

James, D. F., Yogachandran, N., R.Loewen, M., Liu, H. & Davis, A. M. J. 2003 Floc rupture in extensional flow. *J. Pulp and Paper Sci.* **26** (11), 377–382.

Jeffery, G. B. 1922 The motion of ellipsoidal particles immersed in a viscous fluid. *Proc. Roy. Soc. London* **A**, 161–179.

Kao, S. & Mason, S. 1975 Dispersion pf particles by shear. *Nature* **253** (20), 619–621.

Kerekes, R. J. 1995 Perspectives on fibre flocculation in papermakin. In *Int. Paper Physics conf., Niagara*, pp. 23–31.

Kerekes, R. J., Soszynski, R. M. & Tam-Doo, P. M. 1985 The flocculation of pulp fibres. *Proc. The 8th Fundamental Research Symposium, Oxford*. Pulp and Paper Centre, UBC Vancouver, Canada.

Kiviranta, A. & Dodson, C. 1995 Evaluating Fourdrinier formation performance. *J. Pulp Pap. Sci* **21** (11), 379–384.

Lee, C. W. & Brodkey, R. S. 1987 A visual study of pulp floc dispersion mechanisms. *Am. Inst. Chem. Eng. J.* **33** (2), 297–302.

Ljus, C., Johansson, B. & Almstedt, A.-E. 2002 Turbulence modification by particles in a horizontal pipe flow. *Int. J. Multiphase flow* **28** (-), 1075–1090.

Mackaplow, M. B. & Shaqfeh, E. S. G. 1998 A numerical study of the sedimentation of fibre suspensions. *J. Fluid Mech.* **376** (-), 149–182.

Malashenko, A. & Karlsson, M. 2000 Twin wire forming - an overview. In *86th Annual Meeting PAPTAC, Monteral*, pp. A189–201.

Mason, S. G. & Manley, R. S. J. 1957 Particle motion in sheared suspensions: orientations and interaction of ridig rods. *Proc. Roy. Soc. London* **A238**, 117–131.

Matas, J.-P., Morris, J. F. & Guazzelli, E. 2003 Transition to turbulence in particulate pipe flow. *Phys. Review Lett.* **90** (1), 014501–1–4.

Meyer, R. & Wahren, D. 1964 On the elastic properties of three-dimensional fibre networks. *Svensk Papperstidn.* **67** (10), 432–.

Minier, J.-P. & Peirano, E. 2001 The pdf approach to turbulent polydispersed two-phase flows. *Physics report* **352**, 1–214.

Niskanan, K., Kajanto, I. & Pakarinen, P. 1998 *Paper physics*. Fapet OY/Paperi ja Puu Oy.

Norman, B. 1989 Overview of the physics of forming. *Proc. The 9th Fundamental Research Symposium, Oxford*.

Norman, B. & Duffy, G. 1977 Hydrodynamics of papermaking fibres in water suspensions. *Proc. Fibre-water interactions in papermaking, Oxford*.

Norman, B. & Söderberg, D. 2001 Overview of forming literature 1990-2000. *Proc. The 12th Fundamental Research Symposium, Oxford*.

Parsheh, M. 2001 Flow in contractions with application to headboxes. PhD thesis, Dept. of Mechanics, KTH, Stockholm.

Petrie, C. J. S. 1999 The rheology of fibre suspensions. *J. Non-Newtonian Fluid Mech.* **87** (2-3), 369–402.

Pope, S. B. 2000 *Turbulent flows*. Cambrigde University Press.

Rahnama, M., Koch, D. L. & Shaqfeh, E. S. G. 1995 The effect of hydrodynamic interactions on the orientation distribution in a fibre suspension subject to simple shear flow. *Phys. Fluids* **7** (3), 487–506.

Ralambotiana, T., Blanc, R. & Chaouche, M. 1997 Viscosity scaling in suspensions of non-Brownian rodlike particles. *Phys. Fluids* **9** (12), 3588–3594.

Russel, W. B., Hinch, E. J., Leal, L. G. & Tieffenbruck, G. 1977 Rods falling near vertical wall. *J. Fluid Mech.* **83** (2), 273–287.

Schlichting, H. 1999 *Boundary layer theory*. McGraw-Hill.

Schmid, C. F., Switzer, L. H. & Klingenberg, D. 2000 Simulation of fibre flocculation: effect of fiber properties and interfiber friction. *J. Rheology* **44** (4), 781–809.

Segre, P. H., Herbolzheimer, E. & Chaikin, P. M. 1997 Long-range correlations in sedimentation. *Phys Rev Lett* **79** (13), 2574–2577.

Shands, J. 1991 Mechanics of stock jump at jet impingement. *J. Pulp Pap. Sci* **17** (3), 92–99.

Shaqfeh, E. S. G. & Fredrickson, G. H. 1990 The hydrodynamic stress in a suspension of rods. *Phys. Fluids A.* **2**, 7–24.

Shaqfeh, E. S. G. & Koch, D. L. 1988 The effect of hydrodynamic interactions on the orientation of axissymmetric particles flowing through a fixed-bed of spheres or fibres. *Phys. Fluids* **31**, 728–743.

Söderberg, D. 1999 Hydrodynamics of plane liquid jets aimed at applications in paper manufacturing. PhD thesis, Dept. of Mechanics, KTH, Stockholm.

Soszynski, R. M. & Kerekes, R. J. 1988 Elastic interlocking of nylon fibres suspended in liquid, part 2: process of interlocking. *Nordic Pulp and Paper Research J.* **3** (4), 180–.

Steen, M. 1991 Modeling fibre flocculationin turbulent flows: a numerical study. *Tappi J.* **74** (9), 175–181.

Steenberg, B., Olsson, S. & Wahren, D. 1961 Studies on pulp crill. *Svensk Papperstidn.* **64** (17), 634–637.

Steenberg, B. & Wahren, D. 1961 Concentration gradients in boundary layers of streaming fibre suspensions. *Svensk Papperstidn.* **63** (11), 347–355.

Stockie, J. M. & Green, S. I. 1998 Simulating the motion of flexible pulp fibres using the immersed boundary method. *J. Comput. Physics* **147** (1), 147–165.

Stover, C. A., Koch, D. L. & Cohen, C. 1992 Observation of fibre orientation in simple shear flow of semi-dilute suspensions. *J. Fluid Mech.* **238**, 277–296.

Tornberg, A.-K. & Shelly, M. J. 2004 Simulating the dynamics and interactions of flexible fibres in stokes flow. *J. Comput. Physics* **196** (1), 8–40.

Trevelyan, B. J. & Mason, S. G. 1951 Particle motions in sheared suspensions, part i rotations. *J. Colloid Sci.* **6**, 354–367.

Tritton, D. J. 1988 *Physical Fluid Dynamics*. Oxford University Press.

Turnbull, P. F., Perkins, N. C., Schultz, W. W. & Beuther, P. D. 1997 One-dimensional dynamic model of a paper forming process. *Tappi Journal* **80**, 245–252.

Zahrai, S. 1997 On the fluid mechanics of twin-wire formers. PhD thesis, Dept. of Mechanics, KTH, Stockholm.

Åkesson, K. 2004 Floc behaviour in a twin-wire blade pressure pulse. Lic thesis, Div. Paper Tech., Dept. Fibre and Polymer Tech., KTH, Stockholm.

Acknowledgements

During this PhD-project there have been several persons involved, maybe because it covers several fields or simple because it is interesting. However, one person has been endlessly patient and helpful, Dr. Daniel Söderberg.

I have to express my gratitude to Prof. Gustav Amberg, Prof. Henrik Alfredsson and Prof. Fritz Bark at KTH Mechanics for a guiding hand at different stages during the work. Prof. Bo Norman at Div. of Paper Technology, KTH, for comments regarding papermaking. For industrial point of views, I thanks the industrial partners within the network FaxénLaboratoriet and foremost Dr.Lars Martinsson at Albany International AB. My gratitude also goes to Prof. Mark Martinez at Dept. of Chemical and Biological Engineering, University of British Columbia (UBC), Vancouver for guiding me into the field of fibre suspensions and Jean-Pierre Minier at Electricité de France, Paris, for introducing me to two-phase flows. My college Claes Holmqvist is gratefully acknowledged for his contribution in proof-reading my manuscript.

I would also like to thank all my colleagues at KTH Mechanics, without you fluid mechanics would loose one dimension. I want to thank Marcus Gällstedt and Ulf Landén for your helping hands in turning ideas into functional designs. Thanks to my colleagues at UBC for making my stay in Vancouver very pleasant.

Finally I would deeply like to thank my family and dear friends for all their support, love and understanding.

The first part of the project has been performed at FaxénLaboratoriet at KTH Mechanics, with financial support from the industrial partners and VINNOVA. The second part of the project has been funded through the Biofibre Materials Centre (BiMaC) at KTH. The author would like to greatly acknowledge the support from Bengt Ingeströms scholarship fund.

♡ *Phinally Done*